

Influence of Transverse Steel and Casting Direction on Shear Response and Ductility of Reinforced Ultra-High Performance Concrete Beams

Timothy E. Frank, Peter J. Amaddio, Elizabeth D. Decko, Alexis M. Tri, Darcy A. Farrell, Cole M. Landes

Abstract—Ultra-high performance concrete (UHPC) is a class of cementitious composites with a relatively large percentage of cement generating high compressive strength. Additionally, UHPC contains dispersed fibers, which control crack width, carry the tensile load across narrow cracks, and limit spalling. These characteristics lend themselves to a wide range of structural applications when UHPC members are reinforced with longitudinal steel. Efficient use of fibers and longitudinal steel is required to keep lifecycle cost competitive in reinforced UHPC members; this requires full utilization of both the compressive and tensile qualities of the reinforced cementitious composite. The objective of this study is to investigate the shear response of steel-reinforced UHPC beams to guide design decisions that keep initial costs reasonable, limit serviceability crack widths, and ensure a ductile structural response and failure path. Five small-scale, reinforced UHPC beams were experimentally tested. Longitudinal steel, transverse steel, and casting direction were varied. Results indicate that an increase in transverse steel in short-spanned reinforced UHPC beams provided additional shear capacity and increased the peak load achieved. Beams with very large longitudinal steel reinforcement ratios did not achieve yield and fully utilized the tension properties of the longitudinal steel. Casting the UHPC beams from the end or from the middle affected load-carrying capacity and ductility, but image analysis determined that the fiber orientation was not significantly different. It is believed that the presence of transverse and longitudinal steel reinforcement minimized the effect of different UHPC casting directions. Results support recent recommendations in the literature suggesting that a 1% fiber volume fraction is sufficient within UHPC to prevent spalling and provide compressive fracture toughness under extreme loading conditions.

Keywords—Fiber orientation, reinforced ultra-high performance concrete beams, shear, transverse steel.

I. INTRODUCTION

ULTRA-high performance concrete is a cementitious material that is steel fiber-reinforced, typically with a volume of 1% to 3% [1]. It possesses high compressive strength able to exceed 150 MPa [2]. Short, randomly dispersed steel fibers provide tensile strength, encourage pseudo-strain hardening behavior, keep crack widths small at service loads, and facilitate ductility in bending [1]. Steel fibers also prevent spalling, providing UHPC with compressive fracture toughness that exceeds plain concrete [3]. Due to its higher tensile and compressive strength compared to conventional concrete, UHPC has been proposed for multiple applications such as highway overlays, bridge girders, and bridge connection

components. Two main failure modes have been observed in reinforced UHPC (R/UHPC) beams: crack localization or gradual strain hardening of the longitudinal reinforcement. The tensile strength of the UHPC and the strain hardening capacity of the reinforcing bars are two major factors that influence the failure pathway [4]. Strain hardening is the preferred failure path, as the increase in ductility provides a warning before beam failure occurs.

To investigate the shear capacity of R/UHPC beams and the variables that influence their behavior, a pilot study involving two specimens that varied in steel reinforcement ratio was conducted in an unpublished study. One specimen included two 19 mm steel reinforcing bars for a reinforcement ratio of 2.55% and the other specimen included four 13 mm steel reinforcing bars for a ratio of 2.89%. Each specimen had the same transverse steel reinforcement (stirrups spaced equal to the beam's depth) and fiber volume fraction (1%). When subjected to bending via a mid-span point load, both specimens cracked and experienced yield. However, a dominant shear crack formed in one specimen that was not intercepted by a stirrup. The specimen subsequently experienced a fiber bridging failure. Shear cracks also formed in the other specimen, but the dominant crack happened to be bridged by a stirrup, which led to increased ductility, strain hardening in the steel reinforcement, and failure by rebar fracture. It was concluded that transverse steel is critical to providing shear capacity to R/UHPC beams and maximizing the properties of both the UHPC in compression and the steel reinforcement in tension. This study's purpose is to investigate the design variables that influence shear response and capacity of R/UHPC beams in specimens with a relatively high steel reinforcement ratio, a relatively low steel fiber volume fraction, and subjected to high shear demand.

II. LITERATURE REVIEW

Some research has been done on the shear capacity of R/UHPC beams. In one study, when the shear span-to-depth ratio ($a:d$) was 2.26, shear ductility improved by 200% as the transverse steel ratio increased from 0.25% to 0.45% [5]. Not only transverse steel is vital to shear ductility, but it also contributes to crack width control. When a set of R/UHPC beams was tested, crack widths were smaller in the specimens containing transverse steel when compared to ones without

Timothy Frank is with US Air Force Academy, USA (e-mail: timothy.frank@afacademy.af.edu).

transverse steel [6]. Additionally, the presence of transverse steel increased load carrying capacity of the R/UHPC beams.

Longitudinal steel has been shown to affect R/UHPC beam performance. In a comparison of two R/UHPC beams with stirrups spaced at half the beam depth, one was constructed with a reinforcement ratio of 0.96% and the other 2.10%. The beam with the higher reinforcement ratio developed cracks with smaller widths a underwent a larger ductility prior to failure [4].

In addition to steel as transverse and longitudinal reinforcement, randomly disbursed steel fibers are a vital constituent in R/UHPC. One study reported that R/UHPC beams were 350% stronger in shear than those without fibers [2]. In another study of R/UHPC beams with a shear span-to-depth ratio of approximately 2.5, as fibers increased from 0% to 2% by volume, failure mode transitioned from shear to flexural [7]. Crack width control and crushing resistance were found to be sufficient in R/UHPC beams when the fiber volume fraction was as low as 0.5% [8]. A relatively low fiber volume fraction and a relatively high longitudinal steel reinforcement ratio above that recommended for reinforced concrete were determined to be most effective in terms of cost, ductility, and producing warning before failure [8].

Fiber orientation can vary depending on method of placement. In one study comparing unreinforced UHPC beams where placement method varied between parallel and perpendicular to the beam's longitudinal axis, fiber orientation varied between specimens and also varied from what would be expected from a random distribution of fibers [9]. In another study, unreinforced UHPC specimens were cast by pouring UHPC into molds from different locations. It was concluded that specimens cast at the midspan resulted in an increase in fibers near midspan, which aided in crack bridging, and resulted in higher flexural capacity than specimens cast at one end [10]. In tensile specimens, UHPC casting direction has been shown to affect fiber orientation, which directly impacted tensile properties such as first cracking stress, average multi-cracking strength, and strain at localization [11]. Several techniques of evaluating fiber orientation have been reported in the literature including, e.g., high resolution photography of beam cross-sections [9], x-ray computer tomography (CT) analysis [12], and micro-CT scans [8].

III. METHODS

For this experiment, five small-scale R/UHPC beams were cast. A proprietary UHPC pre-mix manufactured by LafargeHolcim, known as DUCTAL, was used for this study. Steel fiber volume fraction and shear span were constant. The steel fibers were 13 mm long and 0.2 mm in diameter. Mix proportions of the constituents are shown in Table I. The standard DUCTAL mix uses 2% steel fibers by volume, however, the specimens in this study only had 1% steel fibers by volume. The intent of reducing steel fibers to 1% follows previous work [8] suggesting a more efficient use of steel within R/UHPC beams may be to increase the amount of longitudinal steel and decrease the amount of steel fibers.

Constituent	kg per m ³
DUCTAL dry premix	2195
Water	115
Superplasticizer	30
Steel Fibers	78

After curing in a warm water-bath for 28 days, the average compressive strength was 97.2 MPa as measured by 73 mm diameter cylinders per [13]. However, we noted that the mix resulted in some specimens and cylinders having suboptimal consolidation, due to a prolonged amount of time taken to adjust the mix to ensure optimal flowability while the material underwent the hydration process. The modulus of rupture was measured to be 13.3 MPa by using a four-point bending test of 101 mm x 101 mm rectangular prisms. Either two or four 19 mm bars were used for longitudinal reinforcement, while 10 mm bars were used for transverse reinforcement. Yield and ultimate strength of the 19 mm bars were 538 MPa and 765 MPa, respectively. Yield and ultimate strength of the 10 mm bars were 876 MPa and 1166 MPa, respectively.

All beams' cross sections were 10.2 cm x 17.8 cm, and length was 67.3 cm (Fig. 1). Two beams were constructed using four 19 mm longitudinal bars (reinforcement ratio, $\rho = 9.5\%$) while three beams had two 19 mm longitudinal bars ($\rho = 4.1\%$), serving as much higher steel reinforcement than typically employed in reinforced concrete design. Transverse steel was spaced at either 111 mm or 68 mm, which was approximately the beam's depth "d" or half the beam's depth "d/2", at or exceeding code limits for reinforced concrete [14]. The shear span-to-depth ratio was either 1.8 or 2.1, depending on the depth to the longitudinal steel, to create shear-dominant beams. The naming convention and test specimen details indicating values of pertinent experimental variables in each of the beams are shown in the testing matrix (Table II).

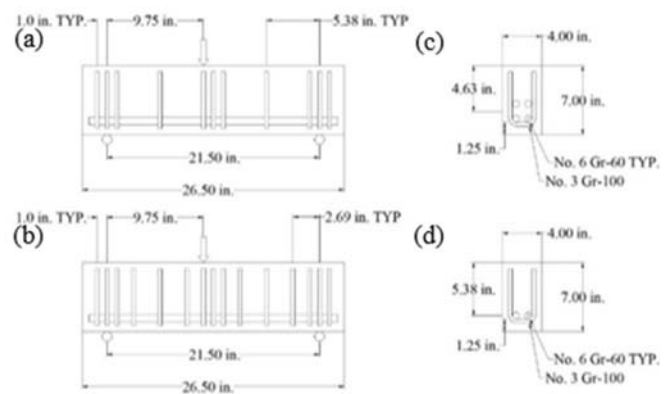


Fig. 1 R/UHPC specimen design showing side view with (a) stirrup spacing of d, (b) stirrup spacing of d/2 and cross-section with (c) $\rho = 9.5\%$ and (d) $\rho = 4.1\%$ (1 in. = 2.54 cm)

Each specimen was monotonically tested under three-point bending at 28 ± 2 days. The loading was off-centered to cause failure on one particular end of the specimen as done in other work, e.g. [15]. The experiment was deflection-controlled at a

rate of 2.54 mm/min and all beams were tested until failure, defined as when the strength dropped under 50% of the peak load observed. Cracking was closely monitored and photographed throughout testing while load and displacement were recorded.

TABLE II
 TEST SPECIMEN DETAILS

Specimen Name	ρ (%)	a:d	Casting Direction	Stirrup Spacing (mm)
4.1-end-d/2	4.1	1.8	end	68
4.1-end-d	4.1	1.8	end	111
4.1-mid-d	4.1	1.8	mid	111
9.5-end-d/2	9.5	2.1	end	68
9.5-mid-d	9.5	2.1	mid	111

IV. RESULTS

Load versus drift results for the five specimens are shown in Fig. 2. Specimen 4.1-end-d/2 was expected to have a high shear capacity due to the close spacing of the transverse reinforcement. During the test, shear cracks formed near 1.8% drift and remained less than 0.3 mm wide due to the bridging capabilities of the steel fibers. The dominant shear crack was apparent at 2.1% drift, but was notably smaller at the location of the stirrup. After reaching its yield strength of 220 kN, multiple shear crack began to form as the load carrying capacity diminished. The load-deflection plot does not indicate strain-hardening occurred in the steel bars, and no crushing in the UHPC was observed. The gradual decrease in post-peak load carrying capacity was due to fiber bridging failure, and ultimate ductility was 4.6% drift. Final cracking patterns of 4.1-end-d/2 and all other specimens are displayed in Fig. 3.

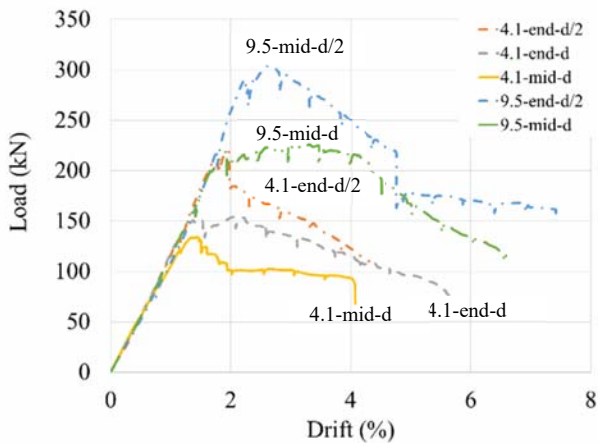


Fig. 2 Load vs. drift

In specimen 4.1-end-d, fewer stirrups were present than in 4.1-end-d/2, so it was suspected to fail by shear prior to reaching its yield strength. The first shear crack appeared at 1.3% drift. By 1.5% drift, the shear crack was noticeably wider as the fibers began to lose their bridging capacity. The peak strength was 154 kN, 53.7% less than the 4.1-end-d/2 as the increased stirrup spacing provided less capacity to support the shear demand. At 2.0% drift, dowel action was vital to providing ductility, and prolonging failure until 4.1% drift.

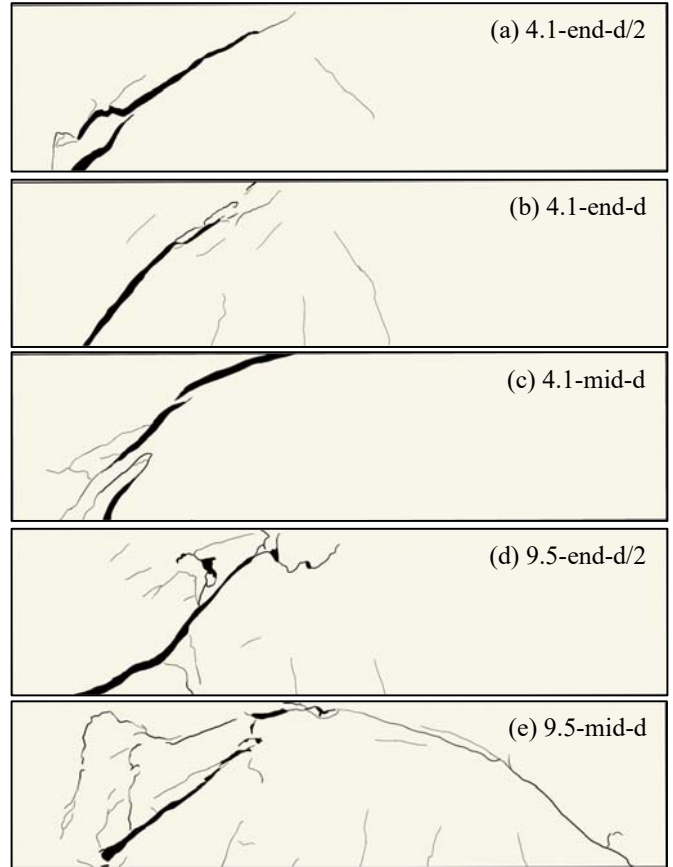


Fig. 3 Final cracking pattern of specimens

Specimen 4.1-mid-d was expected to also fail by shear prior to yield. During testing, the first shear crack was observed at 1.3% drift. By 1.5% drift, fibers began to lose capacity across a dominant shear crack, and the absence of shear reinforcement led to crack localization at the dominate shear crack. The dominant crack prevented other shear cracks from forming. The specimen achieved a peak load of 134 kN. After 2% drift, significant dowel action kept the specimen's load carrying capacity above 50% of peak until 4.1% drift when the specimen failed.

With greater flexural capacity, specimens with a steel reinforcement ratio of 9.5% created a higher shear demand than specimens with the lower reinforcement ratio. As specimen 9.5-end-d/2 began testing, an initial shear cracking was noticed at 2.1% drift. As loading and deflection increased, more shear cracks along with flexural-shear cracks and crushing were observed. Throughout the experiment, the flexural-shear cracks remained under 0.2 mm wide, as they were bridged by the steel fibers. This specimen reached a peak load of 304 kN and no spalling occurred. UHPC's compression fracture toughness kept the compression block intact and facilitated ductility of 7.4% drift.

The first shear crack formed on both spans at 1.2% drift in specimen 9.5-mid-d. As loading increased, some small flexural and flexural-shear cracks formed, and one shear crack became dominant. The longitudinal bars in specimen 9.5-mid-d-1 did not yield, and the specimen achieved a peak load of 226 kN.

After the peak load, strength remained fairly constant until approximately 4.0% drift then decreased linearly until the specimen failed at 6.7% drift.

V. ANALYSIS

When comparing response between specimens, 4.1-end-d/2 had relatively the same strength (220 kN) as 9.5-mid-d (226 kN) but 4.1-end-d/2 was about a third less ductile. Specimen 4.1-mid-d/2 had a lower reinforcement ratio, which reduced shear demand, and closer stirrup spacing, which increased shear capacity relative to 9.5-mid-d. Thus, the stirrups better bridged the dominant shear crack in specimen 4.1-mid-d/2, delaying shear failure and facilitating yield of the longitudinal steel. The specimen with the 9.5% reinforcement ratio experienced more shear cracks and some flexural cracks, which delayed crack localization and facilitated an increase in ductility relative to the specimen with a 4.1% steel reinforcement ratio. While specimen 9.1-mid-d was more ductile, its longitudinal steel never reached yield and thus, the tensile capacity of the longitudinal steel reinforcing bars went underutilized.

Peak load varied inversely with stirrup spacing in specimens at both longitudinal steel reinforcement ratios in this study. Specimen 4.1-end-d/2 achieved 43% more strength than 4.1-end-d, while specimen 9.5-end-d/2 achieved 35% more strength than specimen 9.5-mid-d. Clearly, the increase in transverse steel played a vital role in providing shear capacity, which enabled a larger peak load and higher strength throughout testing. Post-peak strength reduced more quickly in specimens that had a closer stirrup spacing, however results were not conclusive regarding the impact of stirrup spacing on ultimate specimen ductility.

Two nominally identical specimens were tested with a reinforcement ratio of 4.1% and stirrup spacing “d,” but differed in casting direction. Because specimens cast at midspan are expected to have a higher concentration of fibers at midspan [9], fewer fibers were expected in the regions where shear cracks would form when cast in this method. It was hypothesized that more fibers would be present in the shear cracking region in specimen 4.1-end-d, which could delay fiber bridging failure, increase peak strength, and extend specimen ductility. In fact, specimen 4.1-end-d developed more cracks than 4.1-mid-d (Fig. 3), 38.1% more ductility, and a 14.6% higher ultimate strength (Fig. 2). With stirrup spacing so large that shear cracks can form in between them, other mechanisms including dowel action from the longitudinal bars, the uncracked cementitious material, and the embedded steel fibers bridging cracks all contribute to shear capacity. We believe the differing results between response of 4.1-end-d and 4.1-mid-d may underscore both the natural variability in beam response when transverse steel is not provided at a spacing expected to intercept shear cracks, but variations may also be related to differences in the fiber orientation within the specimens.

Fiber orientation was examined by cutting two beams (4.1-end-d, and 4.1-mid-d) transverse to their longitudinal axis at their quarter-points. The cuts facilitated high-resolution photography of the beams’ cross-sections. The cross-sectional area was wet with water to increase the contrast between the

UHPC and steel fibers prior to photography. Image analysis of the photographs was conducted using the commercial software, MATLAB. The image analysis consisted of three steps. First, the color image was converted to a black and white image. White pixels represented the steel fibers and the black pixels represented the UHPC. Each congruent group of white pixels was then bounded by an ellipse. Steel fibers that were oriented perpendicular to the cross-section were bounded by ellipses having similar major and minor axes, or an aspect ratio near 1.0. In contrast, steel fibers that were oriented at an angle to the cross-section resulted in ellipses with a larger aspect ratio. The average aspect ratio of all the ellipses on each cross-sectional photo was calculated. Differences were observed between images. Within specimen 4.1-end-d, for example, the cross-sectional image where the UHPC was cast shows several white ellipses (Fig. 4 (a)), indicating fibers oriented at an angle to the cross-section whereas the mid-span image shows more circular shapes (Fig. 4 (b)).

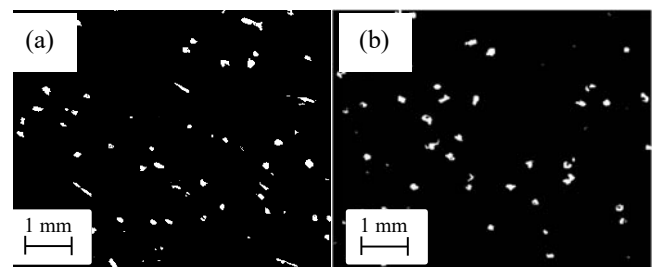


Fig. 4 Images from specimen 4.1-end-d at (a) the end and (b) mid-span

Average aspect ratio of the steel fibers was the metric used to compare fiber orientation along the length of each specimen and between specimens (Fig. 5). The UHPC was cast in the mold at location “C” in specimen 4.1-end-d and at location “B” in specimen 4.1-mid-d. Image analysis shows little difference in average fiber aspect ratio between specimens at the quarter points where the beams were cut. Higher aspect ratios were expected near the location where the UHPC was cast and lower aspect ratios were expected at the other cross sections as the fibers oriented themselves in the direction of the material flow. This expectation was met by specimen 4.1-end-d where the average fiber aspect ratio was 1.82 where UHPC was cast, and decreased as the material flowed along the beam mold towards points B and A where average aspect ratio was 1.77 and 1.76, respectively. However, specimen 4.1-mid-d, cast at mid-span, did not display a higher average aspect ratio at mid-span (location “B”) than the other locations.

Results of image analysis on the average steel fiber aspect ratio between specimens cast at different locations suggest that the casting direction did not make a significant difference on fiber orientation. Previous work investigating fiber orientation mentioned herein [9]-[12] included unreinforced UHPC specimens, however the beams in this study were reinforced with both transverse and longitudinal steel. While there were differences in beam response when casting direction varied (Fig. 2), the presence of steel reinforcement may reduce or

eliminate differences in fiber orientation from casting directions.

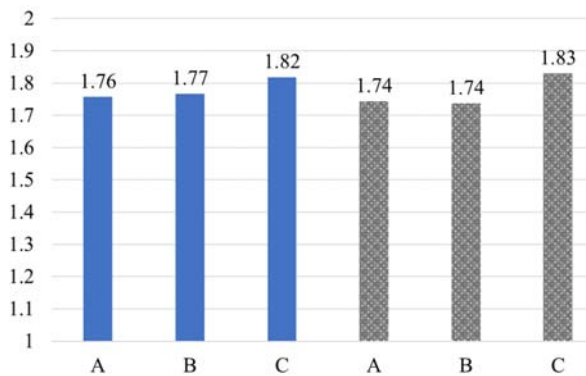


Fig. 5 Steel fiber aspect ratio at various points in specimens 4.1-end-d and 4.1-mid-d

VI. CONCLUSIONS

The purpose of this study was to examine design variables that influence shear response of R/UHPC beams in specimens with a relatively high steel reinforcement ratio, a relatively low steel fiber volume fraction, and subjected to high shear demand. Five small scale beams were constructed and experimentally tested at two reinforcement ratios, two casting directions, and two stirrup spacings.

As expected, all specimens failed in shear. Specimens cast with a smaller stirrup spacing achieved a higher peak load. Stirrups were shown to be more effective at bridging the dominant shear crack than steel fibers alone. The stirrups enhanced the shear strength of the beams and delayed failure.

Only one of the specimens, 4.1-end-d/2, reached yield. Specimens were more likely to utilize the tensile capacity of the steel when they had more closely spaced stirrups and when they had a 4.1% reinforcement ratio than when they were reinforced to 9.5%. None of the specimens failed by crushing of the UHPC, indicating the compressive capacity of the UHPC was not exceeded.

UHPC casting direction did not make a significant difference on fiber orientation to suggest a direct influence. One specimen cast at the end, 4.1-end-d, achieved higher peak load and more ductility than a nominally similar beam cast at mid-span, specimen 4.1-mid-d. However, image analysis did not reveal significant differences in fiber orientation at similar locations along the length of the beam between specimens. The presence of transverse and longitudinal steel reinforcement may have reduced or eliminated the impacts of casting direction. Future research is needed to determine the significance of casting direction on fiber orientation within R/UHPC beams and to correlate response characteristics to fiber orientation.

DISCLAIMER

The views expressed in this paper are those of the authors and not necessarily reflect those of the United States Air Force Academy, the Air Force, the Department of Defense, or the U.S. Government.

ACKNOWLEDGMENT

The authors thank LafargeHolcim and ChromX for their generous donations of DUCTAL material and Grade 100 reinforcement bars, respectively.

REFERENCES

- [1] M. Bermudez, K.-W. Wen, and C.-C. Hung. "A Comparative Study on the Shear Behavior of UHPC Beams with Macro Hooked-End Steel Fibers and PVA Fibers," *Materials* 15, no. 4, February 16, 2022, 1485.
- [2] M. Pourbaba, H. Sadaghian, and A. Mirmiran. "A comparative study of flexural and shear behavior of ultra-high-performance fiber-reinforced concrete beams," *Advances in Structural Engineering* 22, no. 7, May 2019, pp. 1727-1738.
- [3] V. Kodur. "Analysis of Flexural and Shear Resistance of Ultra High Performance Fiber Reinforced Concrete Beams without Stirrups." *Engineering Structures* 174, 2018, pp. 873-884.
- [4] Y. Shao and S. L. Billington. "Utilizing Full UHPC Compressive Strength in Steel Reinforced UHPC Beams," *Second International Interactive Symposium on UHPC*. Iowa State University Digital Press, 2019.
- [5] O. Wang, H.-L. Song, C.-L. Lu, and L.-Z. Jin. "Shear Performance of Reinforced Ultra-High Performance Concrete Rectangular Section Beams." *Structures* 27, October 2020, pp. 1184-1194.
- [6] F. Baby, et al. "Shear Resistance of Ultra High Performance Fibre-Reinforced Concrete I-Beams." *Fract. Mech. Concr. Struct.—High Perform. Fiber Reinf. Concr. Spec. Load. Struct. Appl.*, 2010, pp.1411-1417.
- [7] S. Gomaa, T. Bhaduri, and M. Alnaggar. "Coupled Experimental and Computational Investigation of the Interplay between Discrete and Continuous Reinforcement in Ultrahigh Performance Concrete Beams. I: Experimental Testing." *Journal of Engineering Mechanics* 147, no. 9, September 2021.
- [8] Y. Shao, and S. L. Billington. "Impact of UHPC Tensile Behavior on Steel Reinforced UHPC Flexural Behavior" *Journal of Structural Engineering* 148, no. 1, January 2022, 04021244.
- [9] S.-T. Kang and J.-K. Kim. "Investigation on the Flexural Behavior of UHPC Considering the Effect of Fiber Orientation Distribution," *Construction and Building Materials* 28, no. 1, March 2012, pp. 57-65.
- [10] D.-Y. Yoo, S.-T. Kang, and Y.-S. Yoon. "Effect of Fiber Length and Placement Method on Flexural Behavior, Tension-Softening Curve, and Fiber Distribution Characteristics of UHPFRC," *Construction and Building Materials* 64, August 2014, pp. 67-81.
- [11] B. Graybeal, I. De la Varga, and L. F. M. Duque. "Fiber reinforcement influence on the tensile response of UHPFRC," *First International Interactive Symposium on UHPC*. Iowa State University Digital Press, 2016.
- [12] B. Zhou and Y. Uchida. "Influence of flowability, casting time and formwork geometry on fiber orientation and mechanical properties of UHPFRC," *Cement and Concrete Research* 95, May 2017, pp. 164-177.
- [13] *Standard Practice for Fabricating and Testing Specimens of Ultra-High Performance Concrete*, ASTM C1856, ASTM International, Volume 04.02, West Conshohocken, PA, 2017.
- [14] *Building Code Requirements for Structural Concrete*, ACI 318-19, American Concrete Institute, Farmington Hills, MI, 2019.
- [15] S. Gomaa, and M. Alnaggar. "Transitioning from shear to flexural failure of UHPC beams by varying fiber content," *Second International Interactive Symposium on UHPC*. Iowa State University Digital Press, 2019.